



Bessel Filter

Related terms:

[Amplifier](#), [Butterworth Filters](#), [Chebyshev Filters](#), [Amplitudes](#), [Cutoff Frequency](#), [Passbands](#)

Analog Low-Pass Filters

Marc T. Thompson Ph.D., in [Intuitive Analog Circuit Design \(Second Edition\)](#), 2014

Bessel filter

The Bessel filter (sometimes called the “Thomson” filter) is optimized to provide a constant group delay in the filter passband, while sacrificing sharpness in the magnitude response. Bessel filters are sometimes used in applications where a constant group delay is critical, such as in analog video signal processing. The pole locations for the Bessel filter with a cutoff frequency 1 rad/s are outside the unit circle. Pole locations for an $N = 4$ Bessel filter are shown in Figure 14.19.

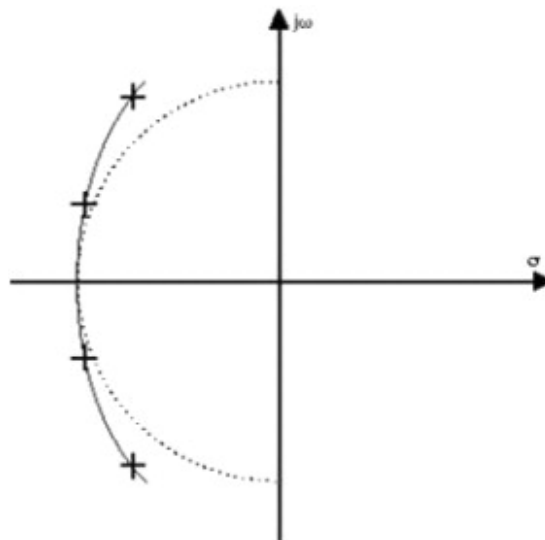


FIGURE 14.19. Pole locations for a Bessel filter, $N = 4$ and cutoff frequency ω_c equal to the radius of the circle.

In Figure 14.20, we see the magnitude response of the Bessel filter for various filter orders. The response is not as sharp as that for the Butterworth filter, with a gradual roll-off in both the passband and stopband. There is little or no overshoot in the step response (Figure 14.21). The group delay exhibits a very flat response in the passband (Figure 14.22).

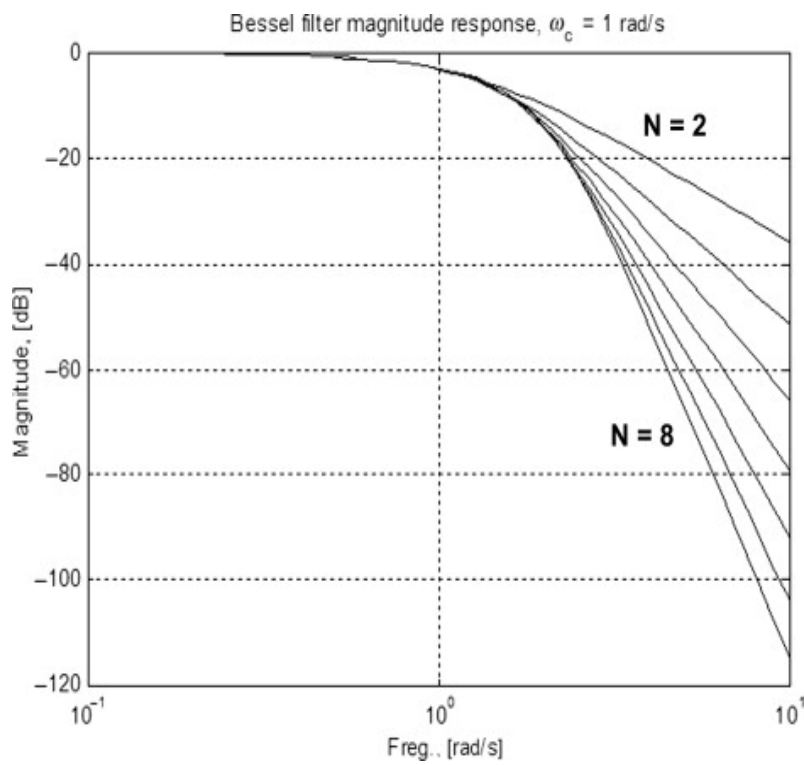


FIGURE 14.20. Bessel filter magnitude response, order $N = 2$ –8, shown for filters with -3 -dB cutoff frequency of 1 rad/s.

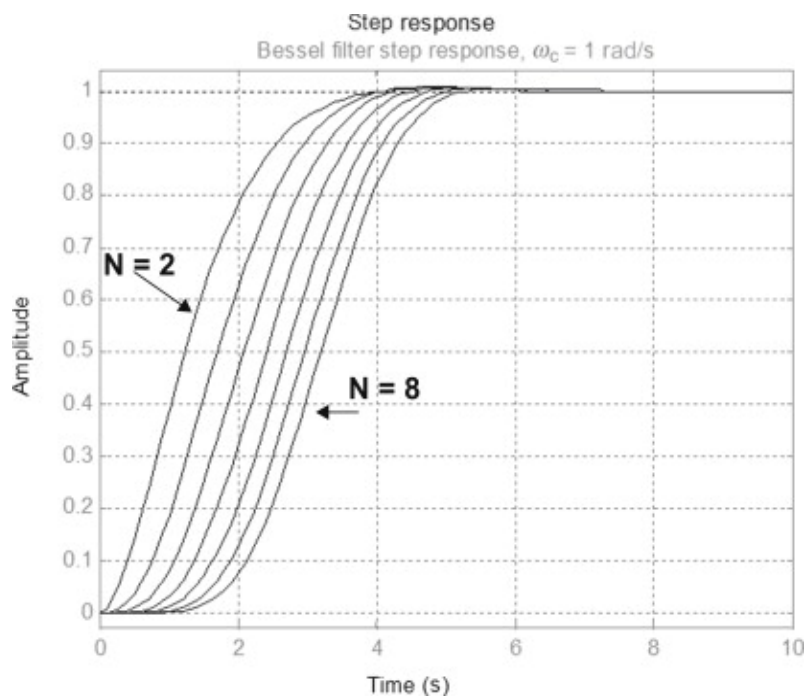


FIGURE 14.21. Bessel filter step response, order $N = 2$ –8, shown for filters with a -3 -dB cutoff frequency of 1 rad/s.

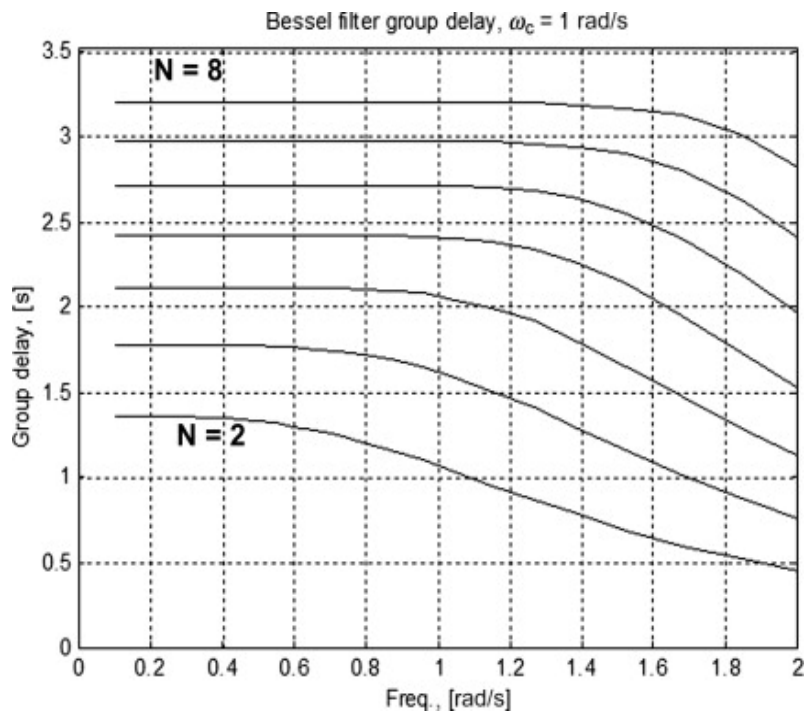


FIGURE 14.22. Bessel filter group delay response, order $N = 2$ –8, shown for filters with a -3 -dB cutoff frequency of 1 rad/s. Note that as the filter order increases, the flatness of the group delay response in the passband improves.

The pole locations for Bessel filters are shown in Table 14.2.

Table 14.2. Pole Locations for Bessel Filters of Varying Filter Orders N , with Filter Cutoff Frequency $\omega_c = 1$ rad/s

N	Real Part ($-\sigma$)	Imaginary Part ($\pm j\omega$)
2	1.1030	0.6368
3	1.0509 1.3270	1.0025
4	1.3596 0.9877	0.4071 1.2476
5	1.3851 0.9606 1.5069 1.5735	0.7201 1.4756 0.3213
6	1.3836 0.9318	0.9727 1.6640
7	1.6130 1.3797 0.9104 1.6853	0.5896 1.1923 1.8375

N	Real Part ($-\sigma$)	Imaginary Part ($\pm j\omega$)
8	1.7627	0.2737
	0.8955	2.0044
	1.3780	1.3926
	1.6419	0.8253

The resultant transfer functions of the Bessel filters are shown in Table 14.3.

Table 14.3. Transfer Function Broken Up into First-Order and Second-Order Quadratic Factors for Bessel Filters of Varying Filter Orders N , with Filter Cutoff Frequency $\omega_c = 1$ rad/s

N	Transfer Function
2	$\frac{1.6221}{s^2 + 2.206s + 1.6221}$
3	$\frac{2.7992}{(s + 1.3270)(s^2 + 2.1018s + 2.1094)}$
4	$\frac{5.1002}{(s^2 + 2.7192s + 2.0142)(s^2 + 1.9754s + 2.5321)}$
5	$\frac{11.3845}{(s + 1.5069)(s^2 + 2.7702s + 2.4370)(s^2 + 1.9212s + 3.1001)}$
6	$\frac{26.8328}{(s^2 + 3.1470s + 2.5791)(s^2 + 2.7672s + 2.8605)(s^2 + 1.8636s + 3.6371)}$
7	$\frac{69.5099}{(s + 1.6853)(s^2 + 3.2262s + 2.9497)(s^2 + 2.7594s + 3.3251)(s^2 + 1.8208s + 4.2052)}$
8	$\frac{198.7746}{(s^2 + 3.5254s + 3.1820)(s^2 + 1.7910s + 4.1895)(s^2 + 2.7560s + 3.8382)(s^2 + 3.2838s + 3.3770)}$

[Read full chapter](#)

URL: <https://www.sciencedirect.com/science/article/pii/B9780124058668000140>

FilterCAD user's manual, version 1.10

Bob Dobkin, Jim Williams, in [Analog Circuit Design](#), 2013

A custom example

For a simple example of how the custom design option works, we'll design a 6th order lowpass Bessel filter by manually entering pole and Q values. When you set the response on the Design screen to "Custom" and press

[Enter]

the usual parameter-entry stage is bypassed and you go directly to the f_0 , Q and f_n section, where you can enter any values you want. We'll use values from Table 23.6, for a filter normalized to $-3\text{db} = 1\text{Hz}$. The published table from which these values were taken didn't mention f_n values at all, so when the author typed them in initially, he left the f_n values as he found them, as zeros. The result was not the desired [lowpass filter](#), but its highpass mirror image. This shows the kind of trap that awaits the unwary.

Table 23.6. f_0 , Q , and f_n Values for 6th Order Lowpass Bessel, Normalized for 1Hz

STAGE	f_0	Q	f_n
1	1.606	0.510	INFINITY
2	1.691	0.611	INFINITY
3	1.907	1.023	INFINITY

Once the values have been entered, they can be re-normalized for any desired corner frequency. Just press

[Enter]

In this case we will re-normalize to 1000Hz, which simply multiplies the f_0 values in the table by 1000.

Looking at the graph of the resulting response (Figure 23.26), we see the characteristic Bessel response, with its droopy passband and very gradual initial roll-off. When we go to the implementation stage, the process is a little different than we are accustomed to. FilterCAD won't optimize a custom design, nor will it specify the mode(s). It will, however, select the device, (the envelope please...) the LTC1164. Now we need to go to the device screen and manually select the mode for each of the three 2nd order sections. We will select mode 3 for all sections, because the three sections each have different corner frequencies, and mode 3 provides for independent tuning of the individual sections by means of the ratio $R2/R4$. (We've seen what the mode 3 network looks like before, so we won't duplicate it here.) Having selected the mode, we can calculate resistor values. The results are shown in Table 23.7.

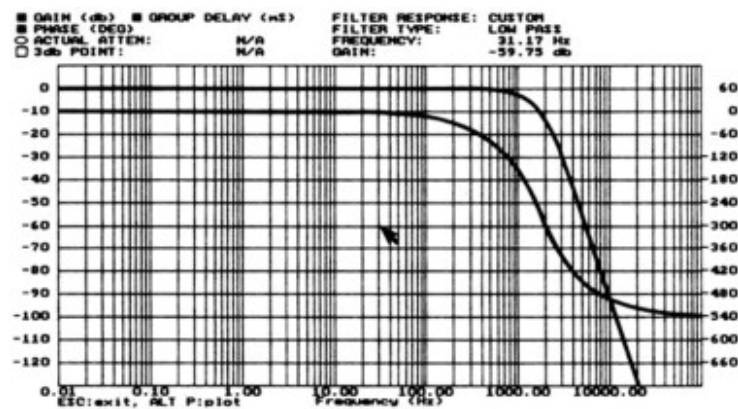


Figure 23.26. 6th Order Lowpass Bessel Response

Table 23.7. Resistors for 6th Order Bessel Lowpass Example

STAGE	R1	R2	R3	R4
1	13.00k	33.20k	10.00k	13.00k
2	10.50k	29.40k	10.00k	10.50k

STAGE	R1	R2	R3	R4
3	10.00k	36.50k	17.40k	10.00k

[Read full chapter](#)

URL: <https://www.sciencedirect.com/science/article/pii/B9780123978882000237>

Analog Filters

Hank Zumbahlen, with the engineering staff of Analog Devices, in [Linear Circuit Design Handbook](#), 2008

Bessel

Butterworth filters have fairly good amplitude and transient behavior. The [Chebyshev filters](#) improve on the amplitude response at the expense of transient behavior. The Bessel filter is optimized to obtain better transient response due to a [linear phase](#) (i.e., constant delay) in the [passband](#). This means that there will be relatively poorer frequency response (less amplitude discrimination).

The poles of the Bessel filter can be determined by locating all of the poles on a circle and separating their imaginary parts by:

$$\frac{2}{n} \quad (8-40)$$

where n is the number of poles. Note that the top and bottom poles are distanced by where the circle crosses the $j\omega$ -axis by:

$$\frac{1}{n} \quad (8-41)$$

or half the distance between the other poles.

The frequency response, group delay, impulse response, and step response for the Bessel filters are cataloged in Figure 8-21. The pole locations and corresponding ω_0 and α terms for the Bessel filter are tabulated in Figure 8-32.

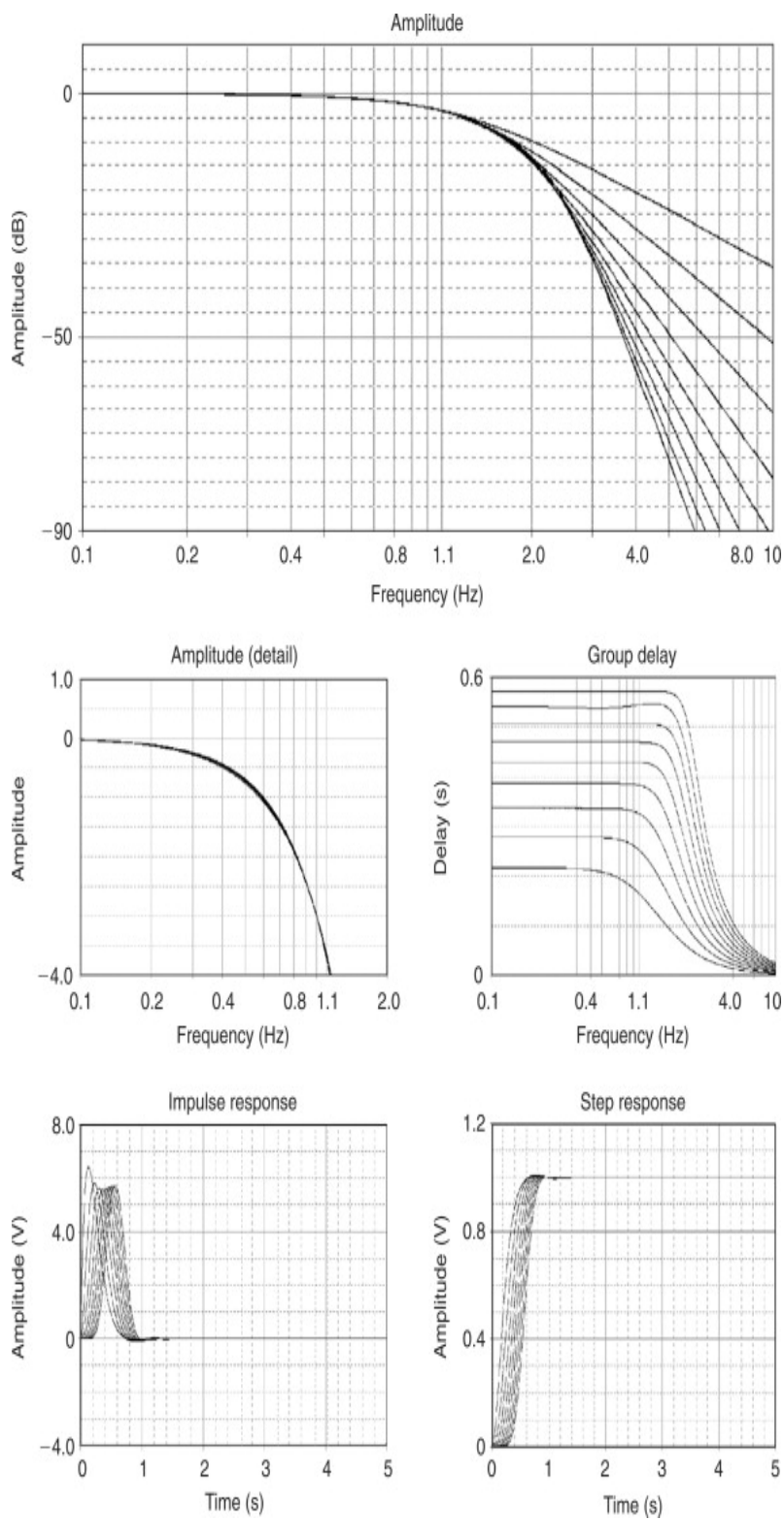


Figure 8-21:. Bessel response

Order	Section	Real part	Imaginary part	F_0	α	Q	-3 dB frequency	Peaking frequency	Peaking level
2	1	1.1050	0.6368	1.2754	1.7328	0.5771	1.0020		
3	1	1.0509	1.0025	1.4524	1.4471	0.6910	1.4185		
	2	1.3270		1.3270			1.3270		
4	1	1.3596	0.4071	1.4192	1.9160	0.5219	0.9705		
	2	0.9877	1.2476	1.5912	1.2414	0.8055		0.7622	0.2349
5	1	1.3851	0.7201	1.5611	1.7745	0.5635	1.1876		
	2	0.9606	1.4756	1.7607	1.0911	0.9165		1.1201	0.7768
	3	1.5069		1.5069			1.5069		
6	1	1.5735	0.3213	1.6060	1.9596	0.5103	1.0638		
	2	1.3836	0.9727	1.6913	1.6361	0.6112	1.4323		
	3	0.9318	1.6640	1.9071	0.9772	1.0234		1.3786	1.3851
7	1	1.6130	0.5896	1.7174	1.8784	0.5324	1.2074		
	2	1.3797	1.1923	1.8235	1.5132	0.6608	1.6964		
	3	0.9104	1.8375	2.0507	0.8879	1.1262		1.5961	1.9850
	4	1.6853		1.6853			1.6853		
8	1	1.7627	0.2737	1.7838	1.9763	0.5060	1.1675		
	2	0.8955	2.0044	2.1953	0.8158	1.2258		1.7932	2.5585
	3	1.3780	1.3926	1.9591	1.4067	0.7109		0.2011	0.0005
	4	1.6419	0.8256	1.8378	1.7868	0.5597	1.3849		
9	1	1.8081	0.5126	1.8794	1.9242	0.5197	1.2774		
	2	1.6532	1.0319	1.9488	1.6966	0.5894	1.5747		
	3	1.3683	1.5685	2.0815	1.3148	0.7606		0.7668	0.0807
	4	0.8788	2.1509	2.3235	0.7564	1.3220		1.9632	3.0949
	5	1.8575		1.8575			1.8575		
10	1	1.9335	0.2451	1.9490	1.9841	0.5040	1.2685		
	2	1.8467	0.7335	1.9870	1.8587	0.5380	1.4177		
	3	1.6661	1.2246	2.0678	1.6115	0.6205	1.7848		
	4	1.3648	1.7395	2.2110	1.2346	0.8100		1.0785	0.2531
	5	0.8686	2.2991	2.4580	0.7067	1.4150		2.1291	3.5944

Figure 8-32:. Bessel design table

[Read full chapter](#)

URL: <https://www.sciencedirect.com/science/article/pii/B9780750687034000080>

IIR Digital Filters

NAZIR A PASHTOON, in [Handbook of Digital Signal Processing](#), 1987

F Analog Filters in Retrospect

Section VI discussed design methods for some popular normalized [analog filters](#). The magnitude responses of all-pole filters such as Bessel, Butterworth, and Chebyshev (type 1) are monotonically decreasing functions of frequency in the stopband. Bessel filters are characterized by a maximally flat group-delay characteristic. [Butterworth filters](#) have a maximally flat magnitude response characteristic. [Chebyshev filters](#), on the other hand, have an equiripple magnitude response characteristic in the [passband](#). For a given order n a [Butterworth filter](#) has a higher attenuation in the stopband and steeper rolloff in the transition band than does a Bessel filter. We can make similar observation between Chebyshev and Butterworth filters. The design tradeoff is between achieving magnitude response specifications with the lowest filter order n and the increased group-delay nonlinearity for the sharper rolloff filter types.

The inverse Chebyshev (Chebyshev type 2) filters have a maximally flat magnitude response in the passband and an equiripple characteristic in the stopband. Inverse Chebyshev filters exhibit a flatter passband magnitude response than does a Butterworth filter of the same order. Flatness is achieved by including the stopband zeros (loss poles) in the transfer function. Inverse Chebyshev filters have sharper

rolloffs than standard Chebyshev filters [21] and have group-delay characteristics more nonlinear than Butterworth filters but less so than standard Chebyshev filters.

The magnitude response of elliptic filters is equiripple in the passband and the stopband and is characterized by the steepest rolloff for a given order n . For example, for $k = 0.75$, $A_p = 2$ dB, and $A_r = 60$ dB, a sixth-order elliptic filter is required. In contrast, a Chebyshev filter of order 10 and a 25th-order Butterworth filter would have to be specified to meet or exceed the given specifications. The group delay of elliptic filters is the most nonlinear, especially near the passband edge. When such sharp rolloffs are desirable and group-delay linearity is a concern, the designer can alleviate the problem by cascading the filter with delay equalizers.

The filters mentioned here are the most frequently used. A broad overview of other filters along with a good selection of nomographs and design curves is available in [31].

[Read full chapter](#)

URL: <https://www.sciencedirect.com/science/article/pii/B9780080507804500096>

Active Filter Design Techniques

Thomas Kugelstadt, in Op Amps for Everyone (Third Edition), 2009

Example 20.1 First Order Unity Gain Low Pass Filter

For a first order unity gain low pass filter with $f_C = 1$ kHz and $C_1 = 47$ nF, R_1 calculates to

$$R_1 = \frac{a_1}{2\pi f_C C_1} = \frac{1}{2\pi \times 10^3 \text{ Hz} \times 47 \times 10^{-9} \text{ F}} = 3.38 \text{ k}\Omega$$

However, to design the first stage of a third order unity gain Bessel low pass filter, assuming the same values for f_C and C_1 , requires a different value for R_1 . In this case, obtain a_1 for a third order Bessel filter from Table 20.7 in Section 20.9 (Bessel coefficients) to calculate R_1 :

$$R_1 = \frac{a_1}{2\pi f_C C_1} = \frac{0.756}{2\pi \times 10^3 \text{ Hz} \times 47 \times 10^{-9} \text{ F}} = 2.56 \text{ k}\Omega$$

When operating at unity gain, the noninverting amplifier reduces to a voltage follower (Figure 20.14), thus inherently providing a superior gain accuracy. In the case of the inverting amplifier, the accuracy of the unity gain depends on the tolerance of the two resistors, R_1 and R_2 .

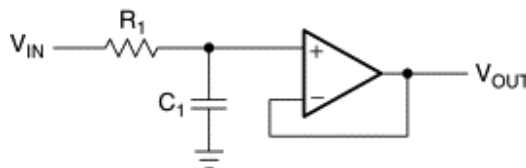


Figure 20.14. First order noninverting low pass filter with unity gain.

[Read full chapter](#)

URL: <https://www.sciencedirect.com/science/article/pii/B978185617505000020X>

Chopper amplifiers complement a DC accurate lowpass filter

Nello Sevastopoulos, in *Analog Circuit Design, Volume Three*, 2015

The LTC1050 is configured as a unity gain 2nd order lowpass filter which center frequency is $(1.2\pi R'C') = 1.72 \cdot f_{\text{CUTOFF}} = 17.2\text{Hz}$ and $Q = 0.5$. Figure 479.2 shows the amplitude response of the filter, and Figure 479.3 shows a well behaved transient response for which Bessel filters are famous. The power supplies used were $\pm 8\text{V}$ to provide a total DC input common-mode range of $\pm 6\text{V}$. The measured wideband noise was $52\mu\text{Vrms}$. The clock, and R, C values of Figure 479.1 can be easily modified to provide a 7th order Butterworth 10Hz filter, such as: $f_{\text{CLK}} = 1\text{kHz}$, $R = 26.7\text{k}$, $C = 1\mu\text{F}$, $R' = 165\text{k}$, $C1 = 0.2\mu\text{F}$ and $C2 = 0.047\mu\text{F}$. The diode at LTC1062 pin 3 should be used to protect the device from incoming signals above the power supplies.

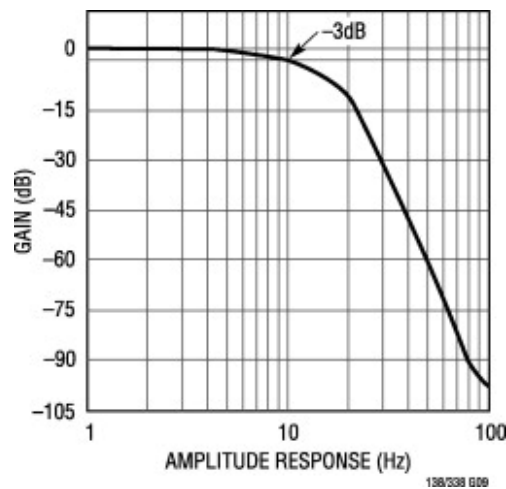


Figure 479.2. Amplitude Response of Figure 479.1, Providing a Close Approximation to a Bessel Filter

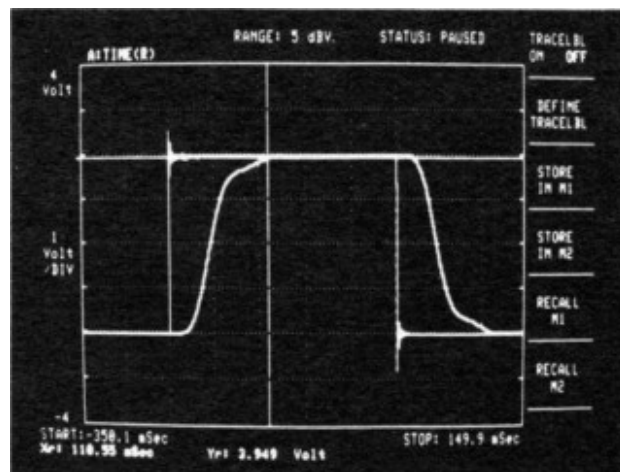


Figure 479.3. Transient Response of the Bessel Lowpass Filter of Figure 479.1

[Read full chapter](#)

URL: <https://www.sciencedirect.com/science/article/pii/B9780128000014004798>

Electronic Design

Michael F. (Mike) Gard, in Developing and Managing Embedded Systems and Products, 2015

Analog semiconductors

While many embedded systems are almost completely digital, every one of them has an analog element or elements to interface with the analog world in which we live. For those systems needing more than a resistive divider, here are some typical examples of analog circuits and their concerns that you may encounter:

- Carefully consider the nature of all analog signal inputs during early design effort. If a sensor provides a bipolar output, I strongly recommend a bipolar power supply for all front-end analog electronics. This avoids DC errors introduced by level shifting and noise introduced by the use of a midrail signal common.
- Amplifiers should have the slew rate necessary to reproduce the highest frequency component in the channel passband at the desired channel gain, but excessive speed is to be avoided. Excessive speed (equivalently, excessive bandwidth) requires extra power from the power source and merely passes along undesired high-frequency noise components which must be filtered out later to limit channel noise.
- Analog filters, especially lowpass filters used in preamplifiers and anti-alias filters, should be based on a Bessel prototype whenever possible. Of the three canonical, all-pole, lowpass prototypes (Butterworth, Chebychev, and Bessel), the Bessel filter is the closest approximation to a linear-phase filter and has the best-behaved impulse and step responses (exhibits the least overshoot and ringing), making the Bessel filter an excellent choice for sampled-data systems.
- Similarly, a Bessel filter prototype is an excellent choice for bandpass or band-reject (notch) filters because of its relatively limited response to impulsive noise. A Sallen–Key implementation is a very good choice for second-order filters or filter sections because it provides relatively uniform response despite variations in the production tolerances of its components.
- Band-reject (notch) filters, particularly filters with high Q, can be difficult to tune; they sometimes exhibit instability problems. Band-reject filters are typically based on twin-tee structures; I suggest an alternative form (Figure 10.17) which is very helpful if a gain-phase analyzer is available to do the tuning. This approach is very stable and can achieve exceptional attenuation at the center frequency. A unity-gain bandpass section is designed to provide the desired Q and center frequency (a Bessel prototype is recommended) and is tuned to provide 180° of phase shift at the center frequency of the notch. The phase-shifted bandpass signal drives an inverting summing amplifier with the other summing amplifier input being the original input to the bandpass filter. Trim the gain of the summing amplifier to be exactly the same as the bandpass filter gain at the center frequency. This arrangement is capable of 100 dBV or better attenuation at the center frequency and is excellent for removing the effects of noise at the power line frequency and low-order harmonics.

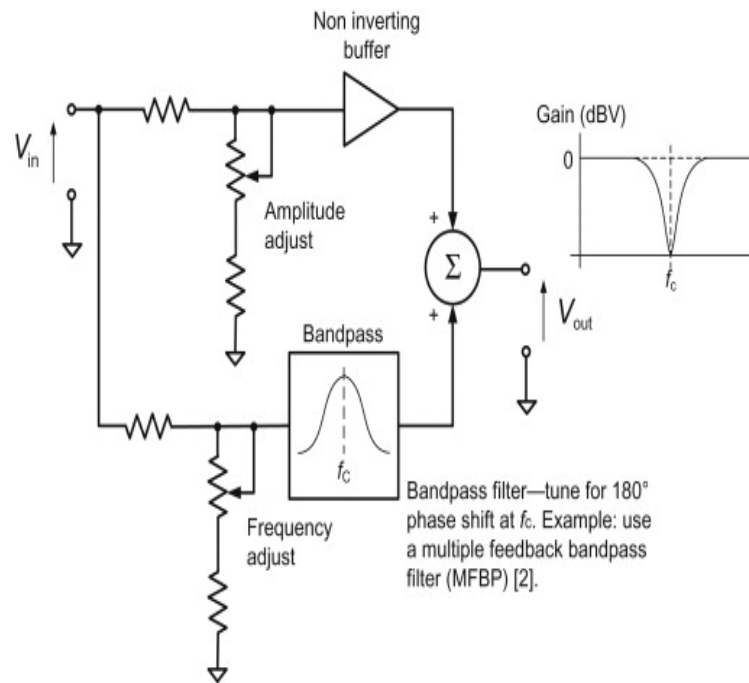


Figure 10.17. Band-reject (notch) filter implementation.

The circuit shown is a stable band-reject (notch) filter implementation which provides simplified tuning, making it easier to use than conventional twin-tee implementations in many applications. Notch characteristics are determined by the bandpass filter design. Depth and center frequency of the notch are affected by tuning accuracy and thermal effects. It is desirable to have independent tuning for amplitude and frequency. Although the tuning elements are shown as conventional potentiometers, this circuit approach is a classic opportunity to improve performance of an embedded system using a dual digital potentiometer to provide the tuning elements.

- A Schmitt trigger is an analog comparator using positive feedback to provide hysteresis around a switching threshold. Schmitt triggers are especially useful as comparators or threshold detectors because they avoid the problem of output switching chatter if the input signal hovers or dithers very near the switching threshold. Two similar structures are possible, depending on whether the designer wishes the signal to go high or low when the input signal exceeds the reference level. The transition thresholds determine the width of the hysteresis window. The reference voltage is the center of the hysteresis window only if the amplifier's positive and negative output saturation voltages are equal in amplitude, which typically requires a bipolar power supply and an amplifier with rail-to-rail output response. If this is not the case, you simply define the desired hysteresis window by identifying the desired transition voltages and then select an appropriate reference voltage knowing the feedback and input resistor values and the amplifier's output saturation voltages (positive and negative). Defining a hysteresis window is especially important if the amplifier is operating from a unipolar power supply. The amplifier output will attempt to swing rail-to-rail (some amplifiers allow true rail-to-rail output; others saturate before reaching the power supply positive and negative rail voltages). Actual output voltages and the input and feedback resistor values determine the Schmitt trigger's switching points. Since Schmitt trigger outputs are essentially digital signals and usually provide a binary input signal to the embedded system's control logic, designs often attenuate and diode clamp the amplifier's output to closely approximate any desired digital logic family (Figure 10.18).

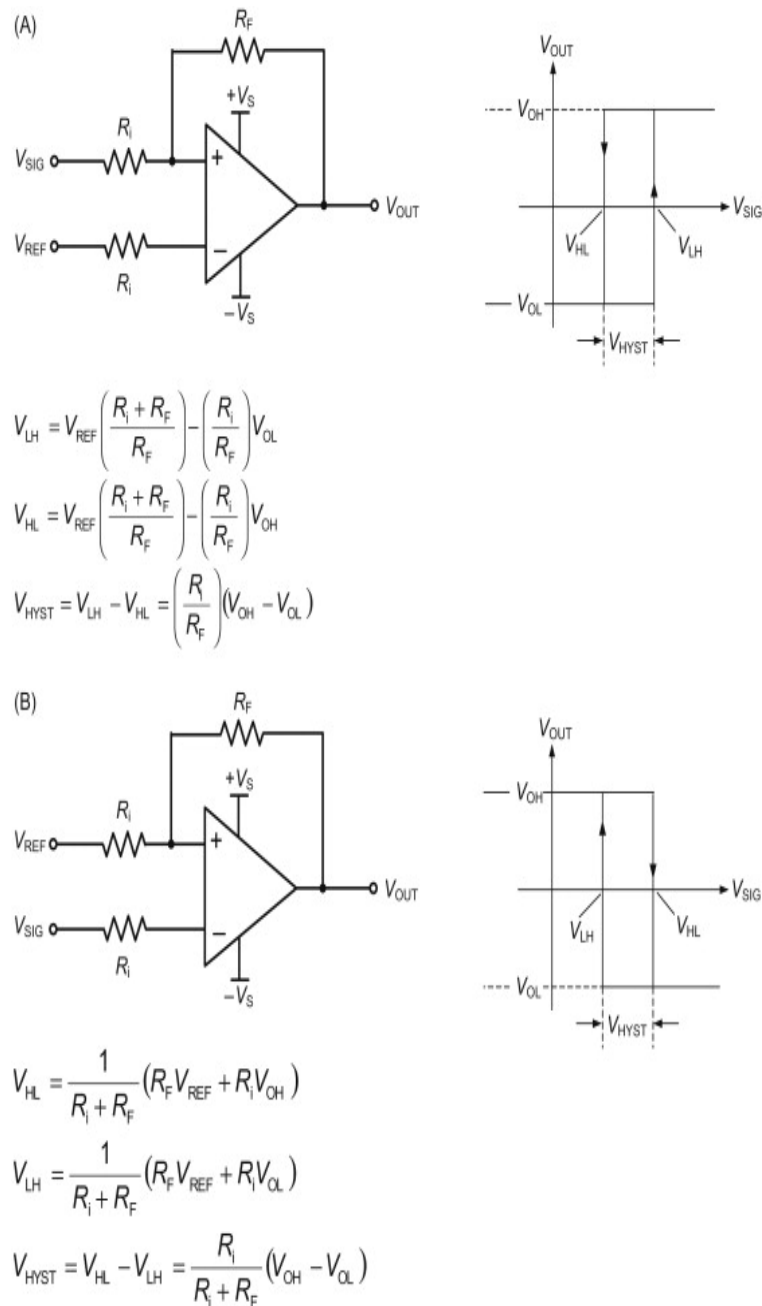
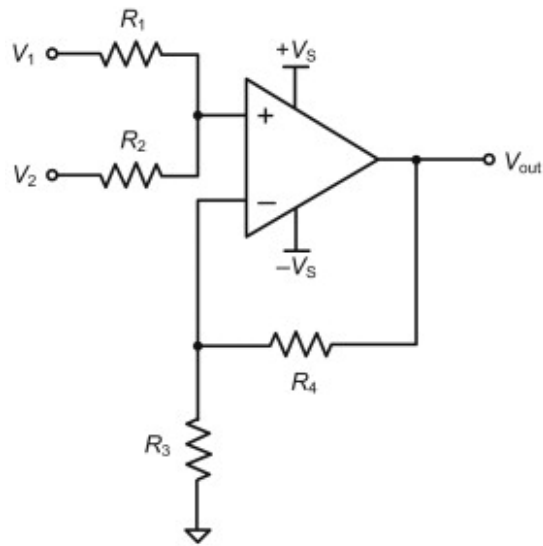


Figure 10.18. (A) and (B): Schmitt-trigger implementations.

In (A), the reference voltage is applied to the inverting input, whereas in (B) the reference voltage is applied to the noninverting input. Notice the effect of output voltage on the switching voltages. This effect is especially pronounced when a unipolar power supply is used and $-V_S=0$.

- Noninverting summers are useful circuit elements for combining signals in a system having only a unipolar power supply. This situation often arises in certain control loop applications. As seen in Figure 10.19, two resistors implement the summing action at the noninverting input while the inverting input and feedback resistances determine the gain.



$$V_{out} = \left(\frac{1}{R_1 + R_2} \right) \left(\frac{R_3 + R_4}{R_4} \right) (R_2 V_1 + R_1 V_2)$$

$$\text{If } R_1 = R_2, \text{ then } V_{out} = \left(\frac{1}{2} \right) \left(\frac{R_3 + R_4}{R_4} \right) (V_1 + V_2)$$

$$\text{If } R_1 = R_2 \text{ and } R_3 = R_4, \text{ then } V_{out} = V_1 + V_2$$

Figure 10.19. Noninverting summing amplifier.

Circuit diagram of a noninverting summing amplifier useful for unipolar and bipolar supply operation. Circuit analysis is readily accomplished by using superposition.

[Read full chapter](#)

URL: <https://www.sciencedirect.com/science/article/pii/B9780124058798000106>

Instrumentation for Low-Noise High-Bandwidth Nanopore Recording

Vincent Tabard-Cossa, in *Engineered Nanopores for Bioanalytical Applications*, 2013

3.5 Noise filtering, sampling, and resolution

Single-molecule studies using nanopores rely on the analysis of ionic current pulses. To obtain information on the structure, dynamics, and kinetics of biomolecules and biological processes under investigation, these electrical pulses must be distinguished from the background noise and statistically analyzed with respect to their depth (ΔI) and duration (Δt) [93,94]. A common way to increase SNR is to attenuate the high-frequency components of the ionic current signal. Reduction of the signal bandwidth is typically achieved by the use of active low-pass filters. Unfortunately, this unavoidably lowers the temporal resolution and distorts the shape of short pulses. This in turn can lead to a loss in structural information or other key biomolecular traits that would have otherwise been observable in the unfiltered data. The amplitude and phase of a signal are affected in different ways by the type of filters and the number of poles used (the larger the

number of poles, the higher the steepness of the roll-off). Butterworth and Bessel filters are the two most commonly used filters. The Bessel filter should be used when studying current signals in the time domain, whereas Butterworth are preferred when analyzing signals in the frequency domain. This is because the former is well behaved in response to transients in the signal but does not provide as sharp a roll-off in the frequency domain (Figure 3.8).

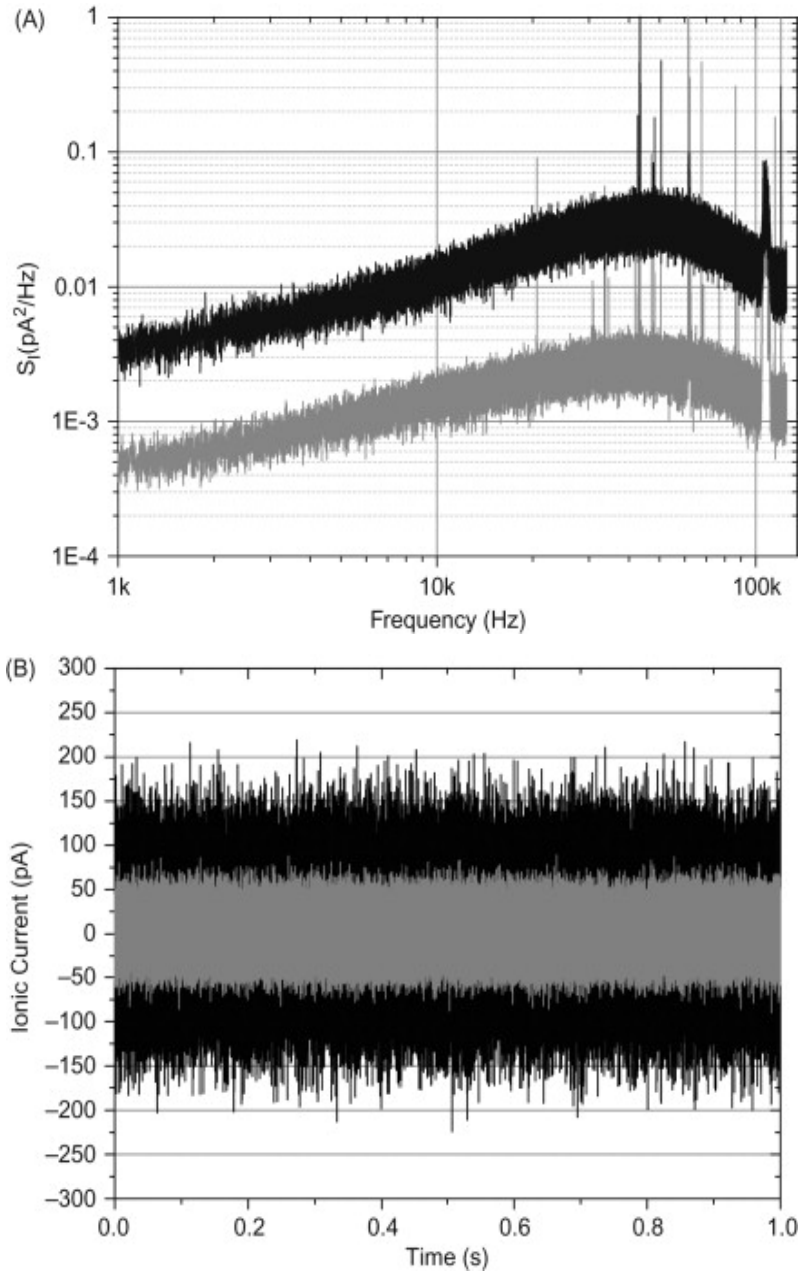


Figure 3.8. (A) Current PSD versus frequency at no applied voltage, low-pass filtered by a 4-pole Bessel filter at 100 kHz for two membranes with no nanopore immersed in 1 M KCl buffered at pH7. The two curves show the difference in high-frequency noise amplitude between a device structure with high (black, >500 pF) and low (gray, <100 pF) input capacitance. The “high” capacitance chip is a 30 nm-thick, 50 μm -wide TEM window, part# NT005X from Norcada mounted as shown in Figure 3.4A. The “low” capacitance chip is painted with a ~ 10 μm layer of PDMS up to ~ 50 μm around the freestanding membrane. (B) Current recording as a function of time, at no applied voltage for the same devices as in (A) illustrating the difference in the current noise.

Choosing the right cutoff frequency, f_c (defined as the frequency at which the signal is reduced by -3 dB, or $1/\sqrt{2}$), depends on the expected duration of the electrical pulses and the minimum acceptable SNR for an experiment. The risetime, τ_{rise} , defined as the time taken for a signal to increase from 10% to 90% of its maximum value, can be expressed for a four-pole Bessel filter (as found in the Axopatch 200B) as:

$$\tau_{\text{rise}} \approx \frac{0.35}{f_c} \quad (3.13)$$

Because of the finite rise time of a filter, the electrical pulse edges of a single-molecule event will be distorted and the pulse amplitude will be attenuated if the pulse duration, $\tau_{\text{event}} \leq 2\tau_{\text{rise}}$. For $f_c=100$ kHz, $\tau_{\text{rise}}=3.5$ μs , such that events <7 μs cannot be accurately detected, with this particular low-pass cutoff frequency. In practice, a few more data points may be necessary to identify with confidence the plateau of the electrical pulse, without *a priori* knowledge of the pulse shape. Recently, Pedone et al. [95] introduced improved criteria to measure the width of short electrical pulses and proposed a method to recover the real pulse height, from the slope of the pulse's falling edge, which renders the identification of a pulse plateau unnecessary for events $\geq 0.2/f_c$. This method can significantly improve the accuracy of the data analysis beyond the usual limitation imposed by electronic filters. Note that many other signal-processing techniques exist, and can be used to accurately recover the pulse width and height of short electrical pulses [12,96], with various degree of complexity, including stochastic analysis using hidden Markov models [97,98], which are outside of the scope of this chapter.

A sufficient number of data points must be acquired to adequately sample the transient electrical pulses resulting from rapid single-molecule events. The choice of sampling frequency is influenced by the particular filter cutoff frequency selected. Any noise in the sampled signal with a frequency component greater than half the digitizing frequency, f_d , will appear in the digitized trace under the alias of lower-frequency noise. In other words, there is a “folding back” of these higher-frequency components into the frequency range from 0 to $f_d/2$ [99]. The Nyquist principle states that this aliasing of the noise is introduced on a signal if the digitizing frequency is not at least twice the filter cutoff frequency:

$$f_d \geq 2f_c \quad (3.14)$$

The minimum sampling frequency is called the Nyquist frequency. In practice however, it is best to set the digitizing frequency significantly higher than the cutoff frequency (e.g., $f_d = 5f_c$ is common). Today's DAQ cards can achieve simultaneous acquisition of multiple signals at 500 kHz sampling frequency with 16-bit resolution, particularly field-programmable gate array (FPGA) based cards.

Analog-to-digital converters (digitizers) can also introduce quantization noise in a current trace. A 16-bit converter with a dynamic range set to ± 10 V, has a quantization step, δ , of $\delta = 20 \text{ V}/2^{16} = 305 \mu\text{V}$. When the quantization is small relative to the signal being measured, the PSD of the quantizing voltage noise can be approximated by [42,84]:

$$S_{\text{digitization}} = \frac{\delta^2}{6f_d} \quad (3.15)$$

According to the equation above, this excess quantization noise arising from digitization is uniformly distributed over the frequency spectrum. This noise can be safely ignored if it is negligible with respect to other sources of noise. One must therefore carefully adjust the dynamic range of the digitizer or use proper gain settings on the amplifier to ensure that the signal being digitized is reasonably large relative to the quantization step.

[Read full chapter](#)

Take the mystery out of the switched-capacitor filter

Richard Markell, in Analog Circuit Design, 2011

What kind of filter do I use? Butterworth, Chebyshev, Bessel or Elliptic

One of the questions most asked among system designers at the shopping malls of America is “how do I choose the proper filter for my application?” Aside from the often used retort, “call Linear Technology,” a discussion of the types of filters and when to use them is appropriate.

A typical application could involve lowpass filtering of pulses. This filter might be in the IF section of a digital radio receiver. The received pulses must pass through the filter without large amounts of overshoot or ringing. A Bessel filter is most likely the filter of choice.

Another application may be insensitive to filter pulse response, but requires as steep a cutoff slope as possible. This might occur in the detection of a series of continuous tones as in an EEG system. If filter ringing is irrelevant, an Elliptic filter may be a good choice.

The trade-offs involved in filter design are critical to the system designer's understanding of this topic. This means understanding what happens in both the time domain and in the frequency domain. At the risk of sounding pedantic, a discussion of this topic is appropriate. A time domain response can be viewed on an oscilloscope as amplitude versus time. It is in the time domain that pulse overshoot, ringing and distortion appear. The frequency domain (amplitude versus frequency) is traditionally where the designer looks at the filter's response (on a spectrum analyzer). A wonderful response in the frequency domain often appears ugly in the time domain. The converse may also be true. It is crucial to examine both responses when designing a filter!

Figures 31.24 through 31.28 reprinted here from Zverev¹⁰ show the time domain step response for the Butterworth, two types of Chebyshev, a Bessel and a synchronously tuned filter. (The synchronously tuned filter is one that is made up of multiple identical stages, but contains no notches. See AM27A for more discussion on this topic.) Figure 31.29 shows the time domain response of the LTC1064-1 8th order Elliptic LP filter to a 10Hz input square wave. The photo shows that a system requiring good pulse fidelity cannot use this filter. Figure 31.30 shows a better filter for this application. It is the LTC1064-3, an 8th order Bessel LPF. The response has a nice, rounded off rise time with no overshoot. The trade-off appears in the frequency domain.

Figure 31.24. Step Response for Butterworth Filters*

Figure 31.25. Step Response for Chebyshev Filters with 0.1dB Ripple*

Figure 31.26. Step Response for Chebyshev Filters with 0.01dB Ripple*

Figure 31.27. Step Response for Maximally Flat Delay (Bessel) Filters*

Figure 31.28. Step Response for Synchronously Tuned Filters*

Figure 31.29. LTC1064-1 Time Domain Response. Filter $f_{\text{CUTOFF}} = 100\text{Hz}$. Input: 10Hz Square Wave. Horiz = 20ms/Div., Vert = 0.5V/Div (Photograph Reproduction of Original)

Figure 31.30. LTC1064-3 Time Domain Response. Filter $f_{\text{CUTOFF}} = 100\text{Hz}$. Input: 10Hz Square Wave. Horiz = 20ms/Div., Vert = 0.5V/Div (Photograph Reproduction of Original)

Figures 31.31 through 31.34 show the frequency domain response of four 8th order filters, the LTC1064-1 through LTC1064-4. (Figure 31.35 shows an expansion of the comparison of the LTC1064-1 and LTC1064-4 roll off from the passband to the stopband.) The LTC1064-1 and LTC1064-4 are 8th order Elliptic filters, while the LTC1064-2 is a Butterworth and the LTC1064-3 is a Bessel. The roll-off from the passband to the stopband is least steep for the LTC1064-3 Bessel filter. This is the price paid for the linear phase response which enable the filter to pass a square wave with good fidelity. Similarly, the LTC1064-2 Butterworth trades slightly worse transient response for steeper roll-off.

Figure 31.31. Frequency Domain Response of LTC1064-1 Elliptic Filter. $f_{\text{CUTOFF}} = 10\text{kHz}$, $V_S = \pm 7.5\text{V}$, LT1007 Output Buffer, 100:1

Figure 31.32. Frequency Domain Response of LTC1064-2 Butterworth Filter.
 $f_{\text{CUTOFF}} = 10\text{kHz}$, $V_S = \pm 7.5\text{V}$, LT1007 Output Buffer, 50:1

Figure 31.33. Frequency Domain Response of LTC1064-3 Bessel Filter. $f_{\text{CUTOFF}} = 10\text{kHz}$, $V_S = \pm 7.5\text{V}$, LT1007 Output Buffer, 75:1

Figure 31.34. Frequency Domain Response of LTC1064-4 Elliptic Filter. $f_{\text{CUTOFF}} = 10\text{kHz}$, $V_S = \pm 7.5\text{V}$, LT1007 Output Buffer, 50:1

Figure 31.35. Frequency Domain Response of LTC1064-1 and LTC1064-4
Transition Region Blow-Up. $f_{\text{CUTOFF}} = 10\text{kHz}$, $V_S = \pm 7.5\text{V}$, LT1007 Output Buffer

The system designer must carefully consider a potential filtering solution in the time and frequency domains. Figures 31.24 through 31.34 are intended as examples to help the designer with this process. There are an infinite variety of filters that can be implemented with switched-capacitor filters to obtain the precise response required for one's system.

Call Linear Technology Applications at (408) 432-1900 for additional help in choosing and/or defining a particularly difficult filtering problem.

The perennial question, “how fast can I sweep?” a filter from one frequency to another can be answered by looking at the transient response curves and renormalizing them to the desired cutoff frequency. Then the settling time can be read off the curve. A frequency sweep is in many aspects like the settling time performance to a pulse point.

Table 31.1 details the four filters mentioned previously and some of their key parameters. Note the wide variation in the stopband attenuation specification. This specification is a measure of the filters steepness of attenuation. This is a key specification for anti-aliasing filters found at an A/D converter's input. Note that for the LTC1064-1 in the figure (corner frequency set to 10kHz) the attenuation to a 15kHz signal would be about 72dB. The Butterworth gives approximately 27dB, while the Bessel only about 7dB attenuation. These latter two filters trade frequency domain roll off for good time domain response.

Table 1. Filter Selection Guide

Part number	Type	Passband ripple	Stopband attenuation	Wideband noise 1Hz – 1MHz	SNR	THD (1kHz)*	Supply
LTC1064-1	Elliptic	$\pm 0.15\text{dB}$	72dB at $1.5f_C$	$150\mu\text{V}_{\text{RMS}}$	1V_{RMS} Input = 76dB	-76dB	V_S $\pm 5'$

Part number	Type	Passband ripple	Stopband attenuation	Wideband noise 1Hz – 1MHz	SNR	THD (1kHz)*	Supply voltage
				165 μ V _{RMS}	3V _{RMS} Input = 85dB	–70dB	V _S ±7.5V
LTC1064-2	Butterworth	3dB	90dB at 4f _C	80 μ V _{RMS}	1V _{RMS} Input = 82dB	–76dB	V _S ±5V
				90 μ V _{RMS}	3V _{RMS} Input = 90dB	–70dB	V _S ±7.5V
LTC1064-3	Bessel	3dB	60dB at 5f _C	55 μ V _{RMS}	1V _{RMS} Input = 85dB	–76dB	V _S ±5V
				60 μ V _{RMS}	3V _{RMS} Input = 94dB	–70dB	V _S ±7.5V
LTC1064-4	Elliptic	±0.1dB	80dB at 2f _C	120 μ V _{RMS}	1V _{RMS} Input = 78dB	–76dB	V _S ±5V
				130 μ V _{RMS}	3V _{RMS} Input = 87dB	–70dB	V _S ±7.5V

*

These specifications from LTC data sheets represent typical values. Optimization may result in significantly better specifications. Call LTC for more details.

[Read full chapter](#)

URL: <https://www.sciencedirect.com/science/article/pii/B9780123851857000317>

Multirate Digital Signal Processing, Oversampling of Analog-to-Digital Conversion, and Undersampling of Bandpass Signals

Lizhe Tan, Jean Jiang, in [Digital Signal Processing \(Third Edition\)](#), 2019

11.4 Application Example: CD Player

Fig. 11.37 illustrates a CD playback system, also described earlier. A laser optically scans the tracks on a CD to produce a digital signal. The digital signal is then demodulated, and parity bits are used to detect bit errors due to manufacturing defects, dust, and so on, and to correct them. The demodulated signal is again oversampled by a factor of 4 and hence the sampling rate is increased to 176.4 kHz for each channel. Each digital sample then passes through a 14-bit DAC, which produces the sample-and-hold voltage signals that pass the anti-image lowpass filter. The output from each analog filter is fed to its corresponding loudspeaker. Oversampling relaxes the design requirements of the analog anti-image lowpass filter, which is used to smooth out the voltage steps.

Fig. 11.37. Simplified decoder of a CD recording system.

The earliest system used a third-order Bessel filter with a 3-dB gain attenuation at 30 kHz. Note that the first-order SDM is added to the 14-bit DAC unit to further improve the 14-bit DAC to 16-bit DAC.

Let us examine the single-channel DSP portion as shown in Fig. 11.38.

Fig. 11.38. Illustration of oversampling and SDM ADC used in the decoder of a CD recording system.

The spectral plots for the oversampled and interpolated signal $\tilde{x}(n)$, the 14-bit SDM output $y(n)$, and the final analog output audio signal are given in Fig. 11.39. As we can see in plot (a) in the figure, the quantization noise is uniformly distributed, and only in-band quantization noise (0–22.05 kHz) is expected. Again, 14 bits for each sample are kept after oversampling. Without using the first-order SDM, we expect the effective ADC resolution due to oversampling to be

Fig. 11.39. Spectral illustrations for the oversampling and SDM ADC used in the decoder of a CD recording system.

$$n = 14 + 0.5 \times \log_2 \left(\frac{176.4}{44.1} \right) = 15 \text{ bits},$$

which is fewer than 16 bits. To improve quality further, the first-order SDM is used. The in-band quantization noise is then shaped. The first-order SDM pushes quantization noise to the high-frequency range, as illustrated in plot (b) in Fig. 11.39. The effective ADC resolution now becomes

$$n = 14 + 1.5 \times \log_2 \left(\frac{176.4}{44.1} \right) - 0.86 \approx 16 \text{ bits}.$$

Hence, 16-bit ADC audio quality is preserved. On the other hand, from plot (c) in Fig. 11.39, the audio occupies a frequency range up to 22.05 kHz, while the DSP Nyquist limit is 88.2 kHz, so the low-order analog anti-image filter can satisfy the design requirement.

[Read full chapter](#)

URL: <https://www.sciencedirect.com/science/article/pii/B9780128150719000117>



Copyright © 2020 Elsevier B.V. or its licensors or contributors.
ScienceDirect® is a registered trademark of Elsevier B.V.

